

Deep level transient capacitance measurements of GaSb self-assembled quantum dots

R. Magno,^{a)} Brian R. Bennett, and E. R. Glaser
Naval Research Laboratory, Washington, DC 20375-5347

(Received 14 February 2000; accepted for publication 22 August 2000)

Deep level transient spectroscopy (DLTS) measurements have been made on GaAs n^+p diodes containing GaSb self-assembled quantum dots and control junctions without dots. The self-assembled dots were formed by molecular beam epitaxy using the Stranski–Krastanov growth mode. The dots are located in the depletion region on the p side of the junction where they act as a potential well that may capture and emit holes. Spectra recorded for temperatures between 77 and 440 K reveal several peaks in diodes containing dots. A control sample with a GaSb wetting layer was found to contain a single broad high temperature peak that is similar to a line found in the GaSb quantum dot samples. No lines were found in the spectra of a control sample prepared without GaSb. DLTS profiling procedures indicate that one of the peaks is due to a quantum-confined energy level associated with the GaSb dots while the others are due to defects in the GaAs around the dots. The peak identified as a quantum-confined energy level shifts to higher temperatures and its intensity decreases on increasing the reverse bias. The activation energy for the quantum-confined level increases from 400 meV when measured at a low reverse bias to 550 meV for a large reverse bias. Lines with activation energies of 400, 640, and 840 meV are associated with defects in the GaAs based on the bias dependence of their peak positions and amplitudes.
 [S0021-8979(00)09622-5]

INTRODUCTION

Self-assembled quantum dots (QDs) have attracted much attention because of interest in studying the basic physics of zero dimensional quantum confined systems and for their potential applications in optoelectronic and electronic devices. From the materials point of view, there are many questions about the details of the growth processes, particularly the Stranski–Krastanov (SK) growth mode,¹ that need to be resolved to narrow the size distribution of the QDs. Little is known about the growth induced defects in the dots and the region around them. These defects may produce nonradiative recombination phenomena that would have a negative impact on the optical properties of the dots. The $\text{In}_x\text{Ga}_{1-x}\text{As}/\text{GaAs}$ QD system is the most intensively studied system because of the interest in developing lasers incorporating them in the active region.^{2,3} High electron mobility transistor⁴ and memory devices⁵ using InAs/GaAs QDs have also been reported. To date little effort has been devoted to GaSb QDs prepared by molecular beam epitaxy (MBE) on GaAs using the SK growth mode. Photoluminescence (PL) experiments have demonstrated that GaSb QDs are significantly different from $\text{In}_x\text{Ga}_{1-x}\text{As}/\text{GaAs}$ QDs as they have a type II band structure with a well in the GaSb valence band, which captures holes, and a barrier in the conduction band, which prevents the capture of electrons.^{6–8} This band structure may be useful in electronic devices, particularly those requiring charge storage.

Space charge techniques such as deep level transient spectroscopy (DLTS),⁹ capacitance–voltage ($C-V$), and

thermally stimulated capacitance have the potential for revealing useful data on quantum-confined states. The subbands of a dot are expected to trap and emit charge in a way that is similar to the trapping and emission processes of point and extended defects that are frequently studied by DLTS. Capacitance techniques may also reveal the presence of non-radiative defects in the dots or the neighboring semiconductor that are not observable in PL spectroscopy. DLTS techniques have already been used to provide data on several other QD systems. A DLTS study of hole energy levels in MBE grown InAs/GaAs QDs identified a peak with an energy of 225 meV as the QDs hole ground state.¹⁰ Lines in the DLTS spectra were also associated with defects in the vicinity of the dots, and some of the defects have displayed metastable behavior.¹⁰ Coulomb charging and electric field stimulated emission have been reported for a DLTS line with an activation energy of 220 meV and identified as the one electron ground state in InP quantum dots embedded in $\text{Ga}_{0.5}\text{In}_{0.5}\text{P}$.^{11,12} An activation energy of 100 meV has been reported for a quantum-confined electron level in $\text{In}_{0.5}\text{Ga}_{0.5}\text{As}$ dots on GaAs.¹³

Optical properties of GaSb QDs have been investigated by PL. The data show a strong emission band near 1.14 eV at low excitation density.^{6,7} This band has been found to shift to higher energy as the excitation power density is increased indicating a type II band structure. Further proof of the type II band structure, with the holes in the GaSb and the electrons in the GaAs, has been obtained by making PL measurements on GaSb dots grown on $\text{Al}_x\text{Ga}_{1-x}\text{As}$ ($x=0.1,0.2$).⁷ Details of the band structure for the GaSb self-assembled dots are difficult to predict as they are dependent upon the strain in the dots and the possible mixing of light and heavy

^{a)}Electronic mail: Magno@bloch.nrl.navy.mil

Report Documentation Page			Form Approved OMB No. 0704-0188		
Public reporting burden for the collection of information is estimated to average 1 hour per response, including the time for reviewing instructions, searching existing data sources, gathering and maintaining the data needed, and completing and reviewing the collection of information. Send comments regarding this burden estimate or any other aspect of this collection of information, including suggestions for reducing this burden, to Washington Headquarters Services, Directorate for Information Operations and Reports, 1215 Jefferson Davis Highway, Suite 1204, Arlington VA 22202-4302. Respondents should be aware that notwithstanding any other provision of law, no person shall be subject to a penalty for failing to comply with a collection of information if it does not display a currently valid OMB control number.					
1. REPORT DATE 14 FEB 2000		2. REPORT TYPE		3. DATES COVERED 00-00-2000 to 00-00-2000	
4. TITLE AND SUBTITLE Deep level transient capacitance measurements of GaSb self-assembled quantum dots				5a. CONTRACT NUMBER	
				5b. GRANT NUMBER	
				5c. PROGRAM ELEMENT NUMBER	
6. AUTHOR(S)				5d. PROJECT NUMBER	
				5e. TASK NUMBER	
				5f. WORK UNIT NUMBER	
7. PERFORMING ORGANIZATION NAME(S) AND ADDRESS(ES) Naval Research Laboratory, Washington, DC, 20375				8. PERFORMING ORGANIZATION REPORT NUMBER	
9. SPONSORING/MONITORING AGENCY NAME(S) AND ADDRESS(ES)				10. SPONSOR/MONITOR'S ACRONYM(S)	
				11. SPONSOR/MONITOR'S REPORT NUMBER(S)	
12. DISTRIBUTION/AVAILABILITY STATEMENT Approved for public release; distribution unlimited					
13. SUPPLEMENTARY NOTES					
14. ABSTRACT					
15. SUBJECT TERMS					
16. SECURITY CLASSIFICATION OF:			17. LIMITATION OF ABSTRACT Same as Report (SAR)	18. NUMBER OF PAGES 7	19a. NAME OF RESPONSIBLE PERSON
a. REPORT unclassified	b. ABSTRACT unclassified	c. THIS PAGE unclassified			

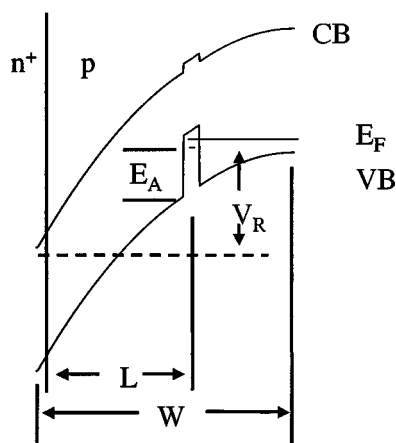


FIG. 1. Schematic of the p^+n junctions with the dots located a distance L from the p^+n interface. W is the depletion width with a bias, V_R , applied. The occupancy of a state with energy E_A is determined by the Fermi energy E_F .

hole bands. Difficulties in modeling the PL data were discussed by North *et al.* who indicated the need for additional techniques for exploring the nature of the GaSb self-assembled dots.¹⁴

A variety of other experiments have been used to examine self-assembled GaSb quantum dots. The MBE growth parameters necessary for the formation of GaSb dots on GaAs have been determined by atomic force microscopy (AFM) measurements,^{15–17} scanning tunneling microscopy,¹⁸ and scanning electron microscopy¹⁹ on uncovered GaSb dots. Transmission electron microscopy measurements have provided information about the sizes of GaSb dots covered by a GaAs cap layer that is used to protect the dots in the PL measurements.^{6,16} Information about the chemical composition of the dots has been obtained by using Raman spectroscopy to measure their phonon modes.^{17,20} Additional confirmation of the barrier to electron capture comes from ballistic electron emission microscopy measurements that place the conduction band of the GaSb dots at 0.08 ± 0.02 eV above the GaAs conduction band.^{21,22}

EXPERIMENTAL DETAILS

A schematic diagram of a junction containing a self-assembled dot is illustrated in Fig. 1 to aid in understanding a DLTS experiment. The measurement consists of monitoring the capacitance C of a diode while applying a reverse bias V_R to set the size of the depletion region W . $C = \epsilon A/W$ where A is the area of the device and ϵ is the dielectric constant. A periodic voltage pulse with a pulse width PW and amplitude PH is also applied to move the energy level E_A above the Fermi level allowing holes to be captured on the dot. Capture rate studies are done by varying the pulse width PW over a time scale that ranges from shorter to longer than the time scale for the capture process. When the bias is returned to V_R the energy level will be moved below the Fermi level, and the trapped holes will make the depletion region a little longer than it was before the filling pulse was applied. The system will return to equilibrium as the trapped holes are emitted, and as this happens the depletion

layer thickness will shrink. Since the emission process changes the thickness of the depletion layer it can be monitored by measuring the time dependence of the capacitance. The emission rate is highly temperature dependent as it is a thermally activated process. The measurement system is set to be sensitive to an emission rate e_R by recording the capacitance at times T_1 and T_2 following the application of the filling pulse. The temperature dependence of $\delta C = C(T_2) - C(T_1)$ is recorded as the spectra. If several energy levels are present each with its own parameters, they each will be observed in a different temperature range in a temperature scan. Most spectra were recorded with a PW of 5 μ s, although some were also recorded with a PW of 1 ms to check that 5 μ s was long enough to fill the energy levels in order to compare peak heights.

The energy level of a state relative to the valence band edge is found by recording spectra for several emission rates and then applying an Arrhenius analysis to the data. It may also be found by fitting the line shape assuming that $\delta C = \delta C_0 \exp(-e_R t)$ where t is the time, and

$$e_R = \sigma_h v_{th} N_v \exp(-E_A/k_B T), \quad (1)$$

where σ_h is the hole capture cross section, v_{th} is the hole thermal velocity, N_v is the density of states at the valence band edge, k_B is the Boltzmann constant, and T is the temperature. This method of extracting an activation energy and capture cross section is difficult for spectra containing several overlapping lines. The discussion above applies to stoichiometric or impurity-related defects distributed spatially in the GaAs, as well as to defects and quantum-confined states associated with the GaSb dots.

Profiling techniques are a useful tool that can be applied to determine whether lines in the spectra are associated with defects distributed through the GaAs, or in the GaSb QDs, or with quantum-confined energy levels on the GaSb QDs. These procedures involve using different combinations of reverse bias and filling pulse height to probe the sample, and may be understood by considering Fig. 1. For a distribution of quantum-confined energy states spatially localized on the dots the bias may be viewed as setting the location of the Fermi energy in the distribution, and the filling pulse as moving the Fermi energy through a small slice of the energy distribution, thereby picking the energy range that will capture and emit charge. Therefore, the peak position of a DLTS line associated with an energy distribution is expected to be bias dependent. A defect with a well defined activation energy E_A but spatially distributed throughout the GaAs will have a peak temperature that is independent of the bias and filling pulse height. If the defect concentration varies with the distance from the n^+p interface, the peak amplitude will change as the region in space being sampled is chosen by the bias and pulse height. For the measurements reported here it is important to remember that using a large bias with a small pulse height will sample a region further from the n^+p interface than the region examined with the same pulse height but a smaller bias. The spectra for defects in the GaSb dots should have a peak position that is independent of bias, and amplitude that depends on the bias and pulse height.

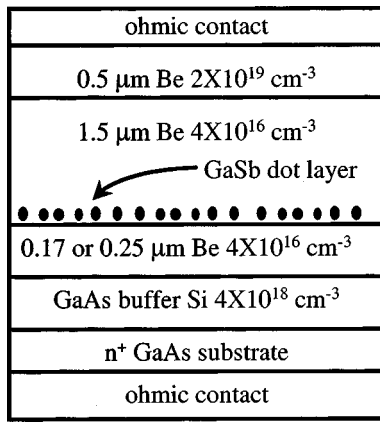


FIG. 2. The layer structure grown on a n^+ GaAs substrate by MBE with the dots located either 0.17 or 0.25 μm from the n^+p interface.

Capacitance–voltage data were also recorded at a variety of temperatures, as this data is necessary to plot the spectra as $\delta C/C_0$ where C_0 is the capacitance at the reverse bias used. $\delta C/C_0$ is proportional to $\rho_{\text{dot}}L/W^2N_a$ where ρ_{dot} is the density of the hole charge emitted from a dot and N_a is the acceptor doping density. Similarly, if N_t is the density of traps distributed through the GaAs then $\delta C/C_0$ is proportional to N_t/N_a . Since $N_a \approx 4 \times 10^{16} \text{ cm}^{-3}$ from the C – V data and the growth conditions, plotting the spectra as $\delta C/C_0$ allows rough comparisons of dot charge and defect concentrations to be made.

The n^+p diodes were prepared by MBE on n^+ GaAs substrates using Si and Be for the n - and p -type dopants, respectively. The GaSb dots were grown on the p side either 0.17 or 0.25 μm from the n^+p interface as indicated in Fig. 2. Additional details of GaSb QD growth are found in Refs. 6, 7, and 15. Two control samples were also prepared. One contained no dots and the other contained a 1 monolayer (ML) GaSb wetting layer. Standard photolithography techniques were used to define ohmic contacts to the p -type GaAs and to define mesas, which were etched to isolate individual devices. An ohmic contact was formed on the backside of the n^+ substrate. A 1 MHz capacitance meter and a dual channel boxcar were used to record the DLTS data presented here.

RESULTS

The MBE growth parameters for the GaSb QDs were mapped by AFM measurements on uncapped QDs^{15–17} as the AFM is unable to examine the QDs buried in the p^+n diodes. An image of a sample formed by depositing 3 ML of GaSb, is presented in Fig. 3 to illustrate the size and distribution of the QDs. The diameter and height of the QDs are $33 \pm 4.0 \text{ nm}$ and $5 \pm 1.3 \text{ nm}$, respectively, and their density ranged between 1 and $2 \times 10^{10} \text{ cm}^{-2}$. QDs were not found by AFM measurements on a sample with a 1 ML GaSb wetting layer. While the energy levels in a single dot may be well defined, the variations in the dot sizes will broaden the observed energy distribution for the quantum-confined levels.

The DLTS data in Fig. 4 illustrate that the two samples containing dots have similar spectra with five prominent

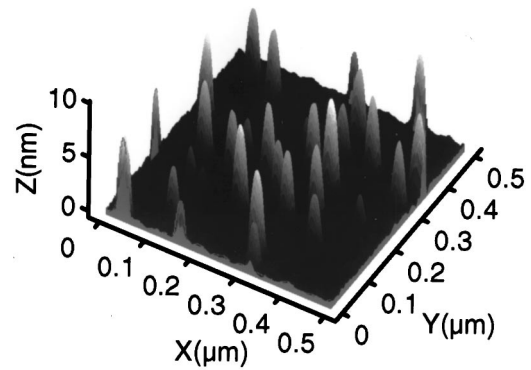


FIG. 3. AFM image of GaSb dots grown on GaAs surface. The diameter and height are $33 \pm 4 \text{ nm}$ and $5 \pm 1.3 \text{ nm}$, respectively, for dots formed by the deposition of 3 ML of GaSb.

peaks that are due to the dot growth as no peaks are found in the spectrum for the control sample without GaSb. To obtain these spectra $V_R = -6 \text{ V}$, $\text{PH} = 6 \text{ V}$, and $\text{PW} = 10 \mu\text{s}$ were used for the sample with the dots located at $L = 0.17 \mu\text{m}$, and $V_R = -8 \text{ V}$, $\text{PH} = 8 \text{ V}$, and $\text{PW} = 5 \mu\text{s}$ were used for the one with the dots located at $L = 0.25 \mu\text{m}$. The need to use different biases and pulse heights to obtain similar spectra is consistent with the dots being at different locations in the two samples. The wetting layer sample, which was grown with 1 ML of GaSb, was measured with $V_R = -5 \text{ V}$, $\text{PH} = 5 \text{ V}$, and $\text{PW} = 5 \mu\text{s}$. It has a broad feature with a peak near 350 K, which is close to a line found in both dot samples. This peak may be due to a defect common to all three samples. Because this peak is found at a high temperature, it is most likely due to a state that is deep in the band gap with a large binding energy. It is not likely to be due to a subband of the quantum well formed by the wetting layer, as a narrow well should have subbands with small binding energies. Spectra were also recorded with $\text{PW} = 1 \text{ ms}$ to check for other lines due to states with smaller capture rates and to determine whether the observed lines were saturated. The 300 K peak for the samples with the quantum dots located $L = 0.17 \mu\text{m}$ and $L = 0.25 \mu\text{m}$ from the n^+p interface increased in intensity by 45% and 25%, respectively, and no other peaks were found when using $\text{PW} = 1 \text{ ms}$ rather than $5 \mu\text{s}$. The data acquired for the Arrhenius analysis presented below were measured with a $\text{PW} = 5 \mu\text{s}$ as it allowed the 251 K peak to be more distinct, and not just a shoulder on the

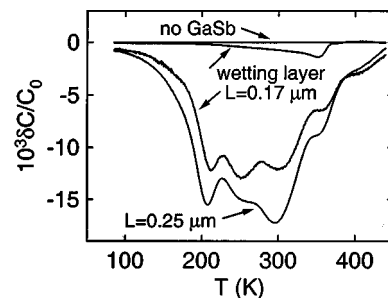


FIG. 4. The DLTS spectra for a control sample with no dots, a sample with a 1 ML GaSb wetting layer, and junctions with the dots at 0.17 and 0.25 μm from the p^+n interface.

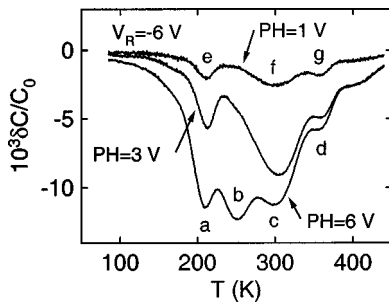


FIG. 5. Profile data with $V_R = -6$ V with filling pulse heights of 1, 3, and 6 V for the junction with $L = 0.17$ μm . The activation energies E_A and the capture cross sections σ_h obtained from an Arrhenius analysis are listed in Table I.

side of the 300 K line. Additional measurements were made on the peaks near 213, 251, and 300 K to determine whether they are associated with the QDs or the GaAs. The line near 400 K in the QD spectra in Fig. 4 is too weak to study in detail.

The series of profile experiments shown in Fig. 5 were performed on the sample with the GaSb dots located 0.17 μm from the n^+p junction by applying a 6 V reverse bias with either a 1, 3, or 6 V filling pulse. The larger the filling pulse height, the closer the layer sampled will be to the dots making it more likely that the dots will capture holes and be observed in the spectra. Capacitance-voltage data measured on the sample indicate that the depletion edge during the filling pulse is about 0.33 μm from the QDs when using $\text{PH} = 1$ V with $V_R = -6$ V. The $\text{PH} = 1$ V ($\text{PW} = 1$ ms) data thus represents a part of the sample that does not include the QDs, and therefore, lines e, f, and g are associated with defects in the GaAs. These three peaks are also found in the spectra for the $\text{PH} = 3$ V ($\text{PW} = 1$ ms) and are labeled a, c, and d in the spectra for $\text{PH} = 6$ V ($\text{PW} = 50$ μs). The increase in amplitude of these lines occurs because more defects are included when the volume sampled is made larger by increasing the pulse height. The defects associated with these three lines may be due either to Sb that has diffused away from the dot region or to stress-induced defects in the GaAs. The peaks at 350 K are near the line in the wetting layer control sample in Fig. 4, and are believed to be associated with defects introduced at the start of the GaSb deposition rather than to quantum-confined energy levels in the QDs. The curve labeled $\text{PH} = 6$ V contains an additional peak, b, near 250 K that represents a new energy level from a part of the sample in the vicinity of the dots.

The data in Fig. 6 for the sample with the dots located 0.25 μm from the n^+p junction were obtained using a variety of biases each with $\text{PH} = 0.5$ V and $\text{PW} = 5$ μs . All four spectra contain a peak near 213 K where the low temperature line is found in the previous figure. With increasing bias the high temperature line for $V_R = -1.5$ V shifts to higher temperatures and becomes broader. Similar spectra were observed when this profiling procedure was used on the sample with the dots at $L = 0.17$ μm , but a somewhat different bias dependence was found for the high temperature peak. The bias dependence may be understood by examining Fig. 1, and assuming the peak is due to quantum-confined energy

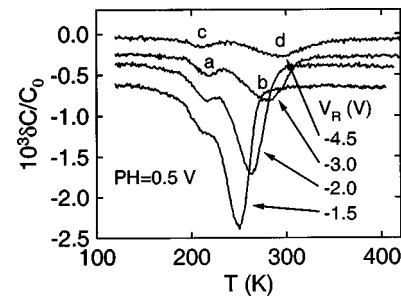


FIG. 6. Profile data for the device with $L = 0.25$ μm using $\text{PH} = 0.5$ V for $V_R = -4.5$ V, -3 V, -2 V, and -1.5 V. The lines are offset vertically by 0.2 for clarity. The activation energies E_A and capture cross sections σ_h are listed in Table II.

levels on a QD. When a large bias is applied, the Fermi level crosses the dots deep in the well so the states sampled will have a large activation energy resulting in a peak at a high temperature. The states sampled with a lower bias will be nearer to the band edge with a smaller activation energy, which will result in a peak at a lower temperature. It would be difficult to explain the peak shifting to a higher temperature with increasing bias assuming a point defect distributed through out the volume of the sample. Typically, a point defect has a peak position that is independent of the bias, or a peak that shifts to lower temperature as the bias is increased because of electric-field-assisted emission processes.

The profiling procedure used to prepare Fig. 6 was used on both QD samples to determine the bias dependence of the peak temperature and amplitude of the high and low temperature peaks shown in Fig. 6. A variety of reverse biases each with $\text{PH} = 0.5$ V were used to make the peak temperature measurements illustrated by the squares, $L = 0.25$ μm , and circles, $L = 0.17$ μm , in Fig. 7. The open symbols demonstrate that the position of the peak near 213 K in both Figs. 5 and 6 is independent of bias, as is expected for a defect distributed throughout the GaAs on top of the QDs. An examination of the intensity of this line in Fig. 5 adds more evidence in support of it being due to a defect in the GaAs. The line is found in the spectra measured with $V_R = -6$ V, and $\text{PH} = -1$ V, which are parameters that sample the GaAs grown on top of the GaSb dots, but not the region near the QDs. In addition, the amplitude of the 213 K line increases in Fig. 5 as larger volumes of the GaAs are included when

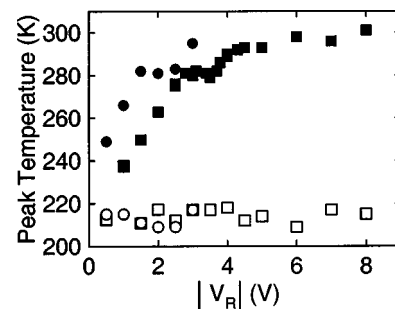


FIG. 7. Dependence of the peak temperature on the magnitude of the reverse bias $|V_R|$ with $\text{PH} = 0.5$ V for both QD samples for: Fig. 5, $L = 0.17$ μm ; \circ line a, \bullet line b; Fig. 6, $L = 0.25$ μm ; \square line a, \blacksquare line b.

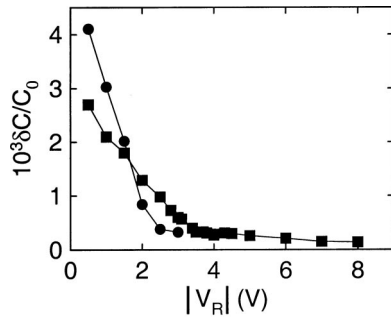


FIG. 8. Peak amplitude dependence on the magnitude of the reverse bias $|V_R|$ with PH=0.5 V for: Fig. 5, $L=0.17 \mu\text{m}$; ● line b; Fig. 6, $L=0.25 \mu\text{m}$ ■ line b.

the pulse height is increased to 3 V and then 6 V. The solid squares in Fig. 7 show the bias dependence of the high temperature peak for the $L=0.25 \mu\text{m}$ sample in Fig. 6, and the closed circles indicate that similar results were obtained for the $L=0.17 \mu\text{m}$ sample in Fig. 5. These curves are consistent with the notion that they are due to similar quantum wells located at different distances from the n^+p junction. The gradual shift of the peak temperature with bias indicates that a band of states is being probed as the bias is increased. Because of the band bending illustrated in Fig. 1, a larger bias is required to obtain a peak at a given temperature for the $L=0.25 \mu\text{m}$ sample (closed squares) than for the $L=0.17 \mu\text{m}$ (closed circles) one. A particular interesting feature is the plateau found near 280 K for $2.8 < |V_R| < 3.5$ for the closed squares and $1.5 < |V_R| < 2.5$ for the closed circles that suggests both sets of QDs have the same energy threshold. The data represented by the closed squares show a transition to a second plateau at 295 K for $|V_R| > 4$ V. Line d in Fig. 6 measured with $|V_R|=4.5$ V is on this second plateau, and thus it may not be due to a quantum-confined level on the quantum dots. While only a single point at $|V_R|=3$ V with a peak temperature of 295 K is shown for the closed circle data, it indicates that a transition to another temperature level is occurring for this sample too.

The amplitude of the high temperature peak for both samples are presented in Fig. 8, and again a bias dependent threshold is found at about 2.5 V for the circles and 3.5 V for the squares. While data are shown for bias values from 4 to 8 V for the closed squares, the low amplitude and width of the peak lead to some uncertainty about its identity, as it may contain a component from the defect associated with peak f in Fig. 5. This peak is expected to be due to a defect in the GaAs grown over the dots in that sample and it may be present here too. A detailed analysis of the amplitude data for biases below the thresholds mentioned above has not been done, but the data suggest an increase in the number of holes captured and emitted as the measurement probes the states closer to the valence band edge.

Activation energies E_A for the peaks labeled a–g in Fig. 5 are listed in Table I, and those for a–d in Fig. 6 are listed in Table II. These were obtained by recording spectra for many emission rates e_R in order to do an Arrhenius analysis using Eq. (1). The energies for lines a and e in Table I are very close to each other and close to the energies for line a

TABLE I. The activation energy E_A and capture cross section σ_h from an Arrhenius analysis of the lines labeled a–g in Fig. 5 for the sample with the QDs at $L=0.17 \mu\text{m}$ from the n^+p interface.

Bias (V)	Pulse height (V)	Line	E_A (meV)	σ_h (cm^2)
–6	6	a	420	1.7×10^{-14}
		b	520	5.1×10^{-14}
		c	610	2.3×10^{-14}
		d	840	5×10^{-13}
–6	1	e	390	4×10^{-15}
		f	640	1.1×10^{-13}
		g	900	5×10^{-12}

and c in Table II suggesting a common defect in both samples. The capture cross section for line a in Table I is different from the other three, but examination of the spectra in Fig. 5 shows that this line is riding on the side of a more intense line making the choice of peak position difficult. Lines d and g in Fig. 5 are also close in energy and have been identified as a defect in the GaAs grown on the GaSb because the bias conditions for g do not sample near the dots. In addition these lines are close to the single line found in the 1 ML GaSb wetting layer control sample. There is no equivalent to the 350 K line of Fig. 5 in Fig. 6. This may reflect the differences in the two profiling methods, or a lower concentration of the 350 K defect in this sample.

Lines b in both Figs. 5 and 6 are found to have very similar activation energies and capture cross sections, and from their behavior in the profile experiments they are identified with a quantum-confined level in the dots. The bias conditions used to measure the activation energy for line b in Fig. 6 were chosen by considering the plateau at a bias of 3 V in Fig. 7 to represent a threshold in the dot's energy distribution. Only the larger QDs are believed to be contributing to peak b in Fig. 6 as an analysis of the amplitude indicates that only about one of every two QDs are emitting holes. Thus, the 550 meV activation energy represents the threshold energy deep in the well. The activation energy of 520 meV for line b in Fig. 5 is somewhat smaller, which may reflect that the dots in this sample are somewhat smaller. Alternatively, this measurement is averaging over a slightly larger energy range in the dots and thus includes holes emitted from shallower energy levels. By considering the band bending in Fig. 1 it is possible to understand that not all energy levels in the dot may be filled with the bias and pulse height combinations used to acquire the data in Fig. 5. If the band bending is large enough only a small band of energies near the bottom of the well may be accessible, and this appears to be the case because 520 meV activation energy is near the

TABLE II. The activation energy E_A and capture cross section σ_h from an Arrhenius analysis of the lines labeled a–d in Fig. 6 for the sample with the QDs at $L=0.25 \mu\text{m}$ from the n^+p interface.

Bias (V)	Pulse height (V)	Line	E_A (meV)	σ_h (cm^2)
–3.0	0.5	a	400	4.5×10^{-15}
		b	550	1.1×10^{-14}
–4.5	0.5	c	380	2.8×10^{-15}
		d	630	1.1×10^{-13}

550 meV found for line b in Fig. 6. The amplitude data in Fig. 8 indicates that at low bias the DLTS is approaching a peak in the dot's distribution of states in energy. To obtain an estimate of the energy distribution, the line shape for the $V_R = -1.5$ V peak in Fig. 6 was fit using the procedures described above to find $E_A = 400$ meV and $\sigma_h = 3.7 \times 10^{-16}$ cm².

Similar activation energies and capture cross sections are found for lines c and f in Fig. 5 and line d in Fig. 6, suggesting that these lines have similar origins. Because line f in Fig. 5 is found for bias and pulse height conditions that do not reach the dots, it is attributed to defects in the GaAs. Similarly, line c in Fig. 5 and d in Fig. 6 are also associated with defects in the GaAs.

DISCUSSION

The DLTS data presented here provide evidence for quantum-confined levels in MBE grown self-assembled QDs, and they demonstrate the introduction of defects in the GaAs during the growth. The dots were located at different positions relative to the n^+p interface to aid in using profiling techniques to separate defects in the neighboring GaAs from features due to the GaSb dots. The spectra for both dot samples contain five discernable peaks, while the control sample with a 1 ML GaSb wetting layer has only a single broad weak DLTS line near 350 K. No DLTS lines are found in the spectra of a control sample without any GaSb. Four of the lines in the QD samples were studied in detail while the fifth was not as it appeared as a weak high temperature shoulder on a more intense line. Three of the lines are identified by the profile measurements as defects in the GaAs in the vicinity of the GaSb dots. One of these three is at the same temperature as the single line found in the 1 ML GaSb wetting layer sample further supporting the notion that it is not due to a quantum-confined level on the QDs. The defect lines found in the dot samples have activation energies and capture cross sections from an Arrhenius analysis that are similar to those reported in the literature.^{23–26} The nature of these is still a topic of discussion, as they are also associated with native defects such as vacancies, interstitials, antisites, and in some cases with impurities such as Cu and Fe. Because the SK growth mode involves the strain-induced movement of GaSb to form quantum dots it is likely that stoichiometric defects will be left in the GaAs near the dots in small quantities measurable in a DLTS experiment. One of the features in the QD spectra is consistent with what is expected for a spatially localized well with a distribution of states in energy.

The bias dependence of the peak temperature and amplitude, illustrated in Figs. 7 and 8, are consistent with what is expected for the DLTS spectra of QDs with a broad distribution of states in energy. An analysis of the amplitude of the $V_R = -3$ V peak in Fig. 6 gives a concentration of 5×10^9 /cm² for the number of holes emitted. This represents less than one hole per dot when compared to $1\text{--}2 \times 10^{10}$ dots/cm² found by AFM measurements. This comparison supports the notion that the 550 meV activation energy represents an energy threshold. The smallest energy as-

sociated with the quantum confined spectra is the 400 meV obtained from the line shape analysis of the $V_R = -1.5$ V data in Fig. 6. An estimate of 2×10^{11} holes/cm² is found for the number of holes that may be trapped in the quantum confined states. This is obtained from an analysis of the amplitude of line b in Fig. 5 where the bias and pulse height conditions are expected to nearly fill the QD. As the AFM measurements give $1\text{--}2 \times 10^{10}$ dots/cm², this count gives an estimate of 10–20 trapped holes on a filled dot. An estimate of the Coulomb charging energy may be found by assuming the quantum dots are disks, as their diameter is large compared to their height. Thus, using $C \sim 8\epsilon d/2$ with $d = 33$ nm, a Coulomb charging energy, q^2/C , of 10.5 meV is found. This is larger than the 7.5 meV calculated using $(550\text{--}400)$ meV/20, but the energy difference $(550\text{--}400)$ meV is an underestimate of the width of the energy distribution in the dots. In this calculation, the threshold energy 550 meV is used for the bottom of the energy distribution and 400 meV (the energy for the $V_R = -1.5$ V data in Fig. 6) is taken for the top, and 20 is assumed for the number of trapped holes. Because of the large distribution in dot dimensions, it is difficult to be more precise than the above calculation. The broad band associated with quantum confinement found here may result from averaging several quantum-confined levels.

A number of PL measurements have been published on GaSb dots made both in this laboratory⁷ and others,^{6,8} and they have associated a PL line at 1.14 eV with the recombination of an electron in the GaAs with a hole in the GaSb. This PL data is consistent with the DLTS reported here. The difference between the GaAs band gap, 1.52 eV, and the 1.14 eV PL energy gives an estimate of 380 meV for the position of the GaSb energy level above the GaAs valence band edge. This is comparable with 400 meV found here for the low bias DLTS peak while the 550 meV DLTS threshold energy corresponds to the long wavelength limit of the PL band.

In conclusion, DLTS has been used to study the formation and properties of GaSb self-assembled QDs grown on GaAs by MBE. The quantum-confined ground state is found to have an energy band that starts near 550 meV above the valence band edge and extends to at least 400 meV from the band edge. The amplitude of the DLTS peak indicates that the quantum-confined band can contain up to 20 holes. The growth of the dots results in the formation of defects in the neighboring GaAs. While the energies of some of these additional lines are similar to lines reported in the literature, the capture cross sections are too different to make conclusive comparisons. The identity of many of the defects is still the subject of research.

ACKNOWLEDGMENTS

The authors thank B. V. Shanabrook and M. E. Twigg for their discussions on the QDs. This work was supported by the Office of Naval Research.

¹I. N. Stranski and L. Krastanov, Sitzungsber. Akad. Wiss. Wien, Math.-Naturwiss. K1., Abt. 2B **146**, 797 (1938).

²N. N. Ledentsov, Semiconductors **33**, 946 (1999) and references therein.

³D. Bimberg *et al.*, Phys. Status Solidi B **194**, 159 (1996).

- ⁴H. Sakaki, G. Yusa, T. Someya, Y. Ohno, T. Noda, H. Akiyama, Y. Kadoya, and G. Noge, *Appl. Phys. Lett.* **67**, 3444 (1995).
- ⁵K. Imamura, Y. Sugiyama, Y. Nakata, S. Muto, and N. Yokoyama, *Jpn. J. Appl. Phys., Part 2* **34**, L1445 (1995).
- ⁶F. Hatami *et al.*, *Appl. Phys. Lett.* **67**, 656 (1995).
- ⁷E. R. Glaser, B. R. Bennett, B. V. Shanabrook, and R. Magno, *Appl. Phys. Lett.* **68**, 3614 (1996).
- ⁸C.-K. Sun, G. Wang, J. E. Bowers, B. Brar, H.-R. Blank, H. Kroemer, and M. H. Pikuhn, *Appl. Phys. Lett.* **68**, 1543 (1996).
- ⁹D. V. Lang, *J. Appl. Phys.* **45**, 3023 (1974).
- ¹⁰M. Sobolev, A. R. Kovsh, V. M. Ustinov, A. Yu. Egorov, and A. E. Zhukov, and Yu. G. Musikhin, *Semiconductors* **33**, 157 (1999).
- ¹¹S. Anand, N. Carlsson, M-E Pistol, L. Samuelson, and W. Seifert, *Appl. Phys. Lett.* **67**, 3016 (1995).
- ¹²S. Anand, N. Carlsson, M-E Pistol, L. Samuelson, and W. Seifert, *J. Appl. Phys.* **84**, 3747 (1998).
- ¹³Z-Q. Fang, Q. H. Xie, D. C. Look, J. Ehret, and J. E. Van Nostrand, *J. Electron. Mater.* **28**, L13 (1999).
- ¹⁴S. M. North, P. R. Briddon, M. A. Cusack, and M. Jaros, *Phys. Rev. B* **58**, 12 601 (1998).
- ¹⁵B. R. Bennett, R. Magno, and B. V. Shanabrook, *Appl. Phys. Lett.* **68**, 505 (1996).
- ¹⁶B. R. Bennett, P. M. Thibado, M. E. Twigg, E. R. Glaser, R. Magno, B. V. Shanabrook, and L. J. Whitman, *J. Vac. Sci. Technol. B* **14**, 2195 (1996).
- ¹⁷B. R. Bennett, B. V. Shanabrook, E. R. Glaser, R. Magno, and M. E. Twigg, *Superlattices Microstruct.* **21**, 267 (1997).
- ¹⁸B. R. Bennett, B. V. Shanabrook, P. M. Thibado, L. J. Whitman, and R. Magno, *J. Cryst. Growth* **175/176**, 888 (1997).
- ¹⁹T. Wang and A. Forchel, *J. Appl. Phys.* **85**, 2591 (1999).
- ²⁰B. R. Bennett, B. V. Shanabrook, and R. Magno, *Appl. Phys. Lett.* **68**, 958 (1996).
- ²¹M. E. Rubin, H. R. Blank, M. A. Chin, H. Kroemer, and V. Narayana-murti, *Appl. Phys. Lett.* **70**, 1590 (1997).
- ²²M. E. Rubin, H. R. Blank, M. A. Chin, H. Kroemer, and V. Narayana-murti, *Physica E (Amsterdam)* **2**, 682 (1998).
- ²³D. Stievenard, X. Boddaert, and J. C. Bourgoin, *Phys. Rev. B* **34**, 4048 (1986).
- ²⁴K. Mallik and S. Dhar, *Phys. Status Solidi B* **184**, 393 (1994).
- ²⁵F. D. Auret, A. W. R. Leitch, and J. S. Vermaak, *J. Appl. Phys.* **59**, 158 (1985).
- ²⁶S. Loualiche, A. Nouailhat, G. Guillot, M. Gavand, A. Laugier, and J. C. Bourgoin, *J. Appl. Phys.* **53**, 8691 (1982).